

# Analysis of Formability on Aerospace Grade Aluminum Alloys

Ms. G . Sraavanthi.

Assistant Professor

Department of Aeronautical Engg,  
Institute of Aeronautical Engineering  
JNTU, Hyderabad, INDIA

Mr. Y. V. Kishore Kumar Nethala.

Assistant Professor

Department of Aeronautical Engg,  
Institute of Aeronautical Engineering  
JNTU, Hyderabad, INDIA

**Abstract - The Aluminum alloys are being used abundantly in aerospace industry because of its excellent mechanical properties and light weight. At present the aluminum alloys contribution in the aerospace industry is increasing to manufacture the aerospace components with better formability and good strength. These components are to be manufactured with a light metal alloy having sufficient strength to bear the strains developed during flight as the development of strains extinct decides component of life (flying hours).**

In the present work, aluminum alloys 6061 and 5052 of aerospace grade has been selected in the study to analyze their formability. The formability of aluminum 6061 is analyzed only for dry condition whereas the formability of aluminum 5052 is analyzed for different tribological conditions such as dry condition, lubricant as grease and annealed condition. The 6061 alloys formability has been compared with 5052 under dry conditions and the present experimental work of A6061 is compared with the existing experimental work of A6061 at same conditions using different methodology.

Further the formability of 5052 aluminum alloy has also been evaluated using lubricant such as grease and annealed condition. The formability under these conditions have been also compared to understand better forming conditions and analyzed for its airworthiness. During the manufacturing (forming) of a component, some stresses are developed and retains with the material. Thus the residual stresses of 5052 have also been analyzed under grease and annealed condition to know the residual stress left over in the material after cupping test (forming of cup). Therefore the effect of stresses is analyzed in a formed component to decide the aerospace component life.

## 1. INTRODUCTION

Aerospace industry requires components of light weight material with high strength. The aluminum and titanium alloys are considered as main materials for aircraft industry. Titanium alloys are very expensive and their formability at room temperature is very low and the forming process for aircraft component production is very costly. Therefore the aluminum alloys are the material which can be considered for the production of components at lower cost.

The advancement of aircraft and rocket technology is directly tied to the advancement and production of aluminum alloys [1]. Aluminum has created the potential for mankind to fly both around the Earth and into space. The airframe of a typical modern commercial transport aircraft is 80 percent aluminum by weight. Aluminum alloys are the overwhelming choice for the fuselage, wing, and supporting structures of commercial airliners and military cargo/transport aircraft. Structural components of current United States Navy aircraft are made of fabricated wrought aluminum.

The aerospace industry demands a lot from the materials it uses. Demands include improved toughness, lower weight, increased resistance to fatigue and corrosion. The boundaries of material properties are being constantly extended as manufacturers strive to give the next generation of aircraft improved performance while making them more efficient. Aluminum is one of the key materials facing these challenges. Aluminum alloy plate is used in a large number of aerospace applications, ranging in complexity and performance requirements from simple components through to primary load bearing structures in aircraft. The first person who managed to understand the potential of aluminum in the aerospace industry was the writer Jules Verne, who provided a detailed description of an aluminum rocket in his novel 'Journey to the Moon' in 1865. In 1903, the Wright brothers got the first airplane off the ground, in which parts of the engine were made of aluminum.

In recent years, demands for aluminum alloy 6061 and 5052 have steadily increased in aerospace, aircraft and automobile applications because of their excellent strength to weight ratio, good ductility, corrosion resistance and cracking resistance in adverse environment.

## 1.1 Introduction Of A6061-T6 And A5052-H32 Alloys:

### 1.1.1 Aluminum 6061-T6 Alloy:



Fig1.1: A6061-T6alloy

Aluminum 6061-T6 alloy is a high strength aluminum alloy, containing magnesium and silicon as its major alloying elements [2]. Originally called "Alloy 61S," was developed in 1935. It has good mechanical properties and exhibits good weld ability. It is one of the most common alloys of aluminum for general purpose use. 6061 aluminum alloy is commonly available in pre-tempered grades such as 6061-O (annealed) and tempered grades such as 6061-T6 (solutionized and artificially aged) and 6061-T651 (solutionized, stress-relieved stretched and artificially aged).

Aluminum 6061-T6 aluminum properties include its structural strength and toughness. It is also offers good finishing characteristics. 6061 aluminum alloy is also easily welded and joined. However, in its -T6 condition the welds may lose some strength, which can be restored by re-heat-treating and artificially aging. Aluminum 6061 alloy has good machinability in harder T4 and T6 tempers. It can be machined in annealed temper. Aluminum 6061 alloy can be easily formed and worked in the annealed condition. The standard methods are used to perform bending, stamping, and deep drawing, and spinning operations. 6061 is more easily worked and remains resistant to corrosion even when the surface is abraded.

### 1.1.2 Aluminum 5052 -H32alloy:



Fig1.2: A5052-H32

Aluminum 5052 alloy is one of the higher strength, non-heat-treatable alloys, which contains magnesium as its major alloying element, with small amounts of chromium, silicon, iron, copper, manganese and zinc. When annealed, alloy 5052 is stronger than the readily available 1100 and 3003 alloys, and stronger than most other 5xxx series alloys. It has good mechanical properties and good workability [3].

The properties of 5052 aluminum include good workability, making it very useful in forming operations. It has very good corrosion resistance, especially to salt water, and can be easily welded. Its high fatigue strength makes it an excellent selection for structures that need to withstand excessive vibrations. Alloy 5052 is commonly used in sheet, plate and tube form. However, this alloy is rated only fair for machinability, so it is not the best choice for extensive machining operations without oil lubricants.

Aluminum alloy 5052's excellent resistance to corrosion makes it particularly well-suited to shipbuilding, fuel tanks and oil lines. Welding 5052 is readily weld able by standard techniques. Heat Treatment Aluminum 5052 is annealed at 345oC, time at temperature and cooling rate are unimportant. Stress relief is rarely required, but can be carried out at about 220oC.

## 1.2applications of A6061 And A5052 Alloys:

### 1.2.1 Aluminum 6061 Alloys:

Al6061 is commonly used for the construction of aircraft structures, such as wings and fuselages, more commonly in homebuilt aircraft than commercial or military aircraft. The typical applications of 6061 alloy include aircraft and aerospace components, brake components, valves, marine fittings, driveshaft.

Other common applications of aluminum 6061 alloy include tank fittings, heavy duty structures, truck and marine components, pipelines railroad cars and general structural and high pressure applications.

### 1.2.2 Aluminum 5052 Alloy:

The aluminum 5052 has a great application in the aircraft industry such as aircraft control surfaces, aircraft landing gear doors, aircraft leading edges and trailing edges. This alloy is used for the manufacture of fuel tanks, missile wings, fuselage components and helicopter rotor blades. 5052 alloy also has a good application in the aircraft flooring, navy bulkhead joiner panels, fan casing fuel cells, engine nacelles, marine and naval panels, advanced energy absorbers and in the high performance composite structure.

Other common applications for aluminum alloy 5052 include aircraft fuel and oil lines, hydraulic tubes, heat exchangers, pressure vessels, appliances like home freezers, kitchen cabinets, fencing, lighting, wiring and rivets. It is regularly used in general sheet metal work.

### 1.3 material Properties of Aluminum 6061 And 5052

#### Alloys:

##### 1.3.1 Physical Properties:

TABLE 1.1: PHYSICAL PROPERTIES OF A6061-T6 AND A5052-H32 ALLOYS:

PROPERTY	Al 6061 ALLOY	Al5052 ALLOY
DENSITY	2.70g/cm <sup>3</sup>	2.68g/cm <sup>3</sup>
MELTING POINT	650degC	605 degC
THERMAL EXPANSION	23.4*10 <sup>-6</sup> /k	23.7*10 <sup>-6</sup> /k
MODULUS OF ELASTICITY	70GPa	70GPa
THERMAL CONDUCTIVITY	166W/m.k	138W/m.k
ELECTRICAL RESISTIVITY	0.040*10 <sup>-6</sup> Ω.m	0.0495*10 <sup>-6</sup> Ω.m

##### 1.3.2 Chemical Composition:

Table 1.2: Chemical Composition Of A6061-T6 And A5052-H32 Alloys:

Alloy	Mg	Cr	Fe	Si	Mn	Zn	Cu	Others
6061	0.80	0.04	0.0	0.40	0.0	0.0	0.15	0.0-0.15
	-	-	-	-	-	-	-	-
	1.20	0.35	0.7	0.80	0.1	0.2	0.40	
	0		0		5	5		
5052	2.20	0.15	0.0	0.0-0.25	0.0	0.0	0.0-0.10	0.0-0.15
	-	-	-	-	-	-	-	-
	2.80	0.35	0.4		0.1	0.1		
	0		0		0	0		

##### 1.3.3 Mechanical Properties:

Table 1.3: Mechanical Properties Of A6061-T6 And A5052-H32 Alloys:

PROPERTY	Al 6061 ALLOY	Al5052 ALLOY
Ultimate tensile strength,psi	45,000	33,000
Yield strength,psi	40,000	28,000
Brinell hardness	90	60

#### 1.4 FORMABILITY :

Formability is the measure of the amount of deformation a material can withstand prior to fracture or excessive thinning. Formability is a term applicable to sheet metal forming. Sheet metal operations such as deep drawing, cup drawing, bending etc involve extensive tensile deformation. Therefore, the problems of localized deformation called necking and fracture due to thinning down are common in many sheet forming operations [4].

Formability is the ease with which a sheet metal could be formed into the required shape without undergoing localized necking or thinning or fracture. When a sheet metal is subjected to plane strain deformation, the critical strain, namely, the strain at which localized necking or plastic instability occurs can be proved to be equal to  $2n$ , where  $n$  is the strain hardening exponent. For uniaxial

tensile loading of a circular rod, the critical or necking strain is given to be equal to  $n$ . Therefore, if the values of  $n$  are larger, the necking strain is larger, indicating that necking is delayed.

In some materials diffuse necking could also happen. Simple uniaxial tensile test is of limited use when we deal with formability of sheet metals. This is due to the biaxial or triaxial nature of stress acting on the sheet metal during forming operations. Therefore, specific formability tests have been developed, appropriate for sheet metals. Loading paths could also change during sheet metal forming. This may be due to tool geometry.

#### 1.5 Methods of Formability Testing:

##### 1.5.1 Erichsen Cupping Test:

The Erichsen cupping test is ductility, which is employed to evaluate the ability of metallic sheets and strips to undergo plastic deformation in stretch forming. The test consists of forming an indentation by pressing a punch with a spherical end against a test piece clamped between a blank holder and a die, until a through crack appears. The depth of cup is measured [5].

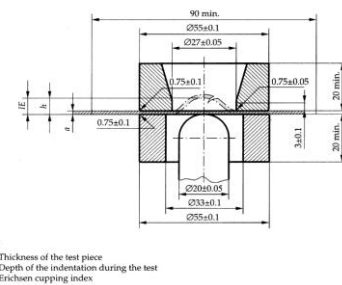


Fig 1.3: Erichsen test Punch and Die

The Erichsen cupping test is used to assess the stretch formability of sheets. This test can be classified as a stretch forming test which simulates plane stress biaxial tensile deformation. For the Erichsen test a sheet specimen blank is clamped firmly between a blank holder which prevents the in-flow (feeding) of sheet volume from under the blank holder into the deformation zone during the test. The standardized dimensions of the test set-up are shown in Figure 1.3. The ball punch is forced onto the sheet specimen till cracks begin to appear in the bulge dome. The distance the punch travels is referred to as the Erichsen drawing index IE (index Erichsen) and is a measure for the formability of the sheet during stretch forming.

##### 1.5.2 Erichsen Index:

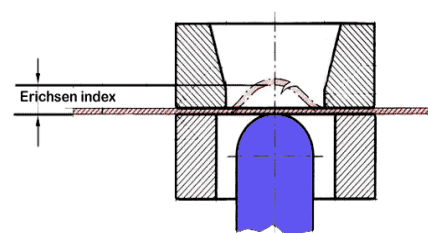


Fig 1.4: Erichsen Index

It is used to determine the metal's suitability for the metal-forming technique called "drawing." The sheet metal to be tested is clamped between two dies, and a punch with a hemispherical end is forced into it at a slow, controlled speed until the metal cracks.

The test is conducted by supporting the sheet on a circular ring and deforming it at the center of the ring by a spherical pointed tool. The depth of impression (or cup) in mm required to obtain fracture is the Erichsen value for the metal. Erichsen standard values for trade qualities of soft metal sheets are furnished by the manufacturer of the machine corresponding to various sheet thicknesses.

#### 1.5.3 Deep Drawing Method:

Deep drawing is a sheet metal forming process in which a sheet metal blank is radially drawn into a forming die by the mechanical action of a punch. It is thus a shape transformation process with material retention. The process is considered "deep" drawing when the depth of the drawn part exceeds its diameter. This is achieved by redrawing the part through a series of dies. The flange region (sheet metal in the die shoulder area) experiences a radial drawing stress and a tangential compressive stress due to the material retention property. These compressive stresses (hoop stresses) result in flange wrinkles (wrinkles of the first order). Wrinkles can be prevented by using a blank holder, the function of which is to facilitate controlled material flow into the die radius [6].

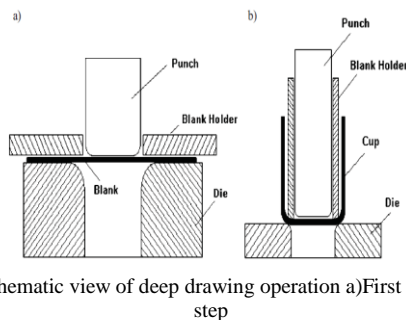


Fig 1.5 Schematic view of deep drawing operation a)First step b) Next step

#### 1.5.4 Limit Dome Height Method:

This method combines advantageous of simulating tests and of the forming limit diagram. Based on observations by Drewes gosh proposed to represent the heights of the parts as functions of the minimum strains occurring in rectangular specimens (of Nakazima type) stretched on a hemispherical punch until fracture [6]. By drawing a curve through the experimental points obtained with specimens of different width.

The method has been modified by English researchers under the name of strip stretch test and by American researchers, named limiting dome height test. The height of the corresponding to plane strain is a formability index denoted by LDH<sub>0</sub>. This is the minimum compared to the heights obtained for other states of strain. The width of the specimen corresponding to plane strain is a characteristic of the material. In spite of its advantages the method has been little used in industry due to the large

dispersion of the LDH<sub>0</sub> values and the large amount of the experimental work.

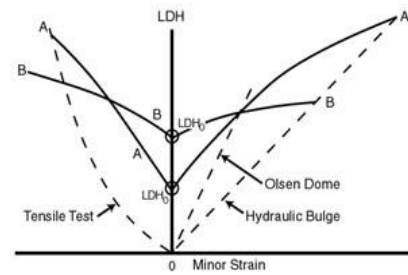


Fig 1.6: Schematic showing LDH curves

#### 1.5.5 Marciniak Test:

In deep drawing with a flat bottom punch tearing of part usually occurs at the connection between the bottom and the cylindrical wall. In order to produce the tearing at the planar bottom of the cup, Marciniak proposed to use the hollow punch and an intermediate part having a circular hole placed between punch and work piece. The obtention of different strain paths is ensured by using punches with different cross sections (circular, elliptical, rectangular) [6].

The advantage of this test is that tearing appears at the planar bottom of the part thus eliminating the errors of measurement caused by a curvature. Disadvantages are the complex shapes of punch and die and the limitations of the tests the positive domain of the forming limit curve. In order to overcome these drawbacks the test can be modified by using specimens and intermediate parts having different shapes. By varying the radius of the recesses the entire domain of the FLD is obtained using only one ring punch.

#### 1.6 Forming-Limit Diagram (FLD):

The first forming limit diagram was published by Keeler in 1961. But he determined the forming limit curve only in the positive range of minor strain. The left hand side was then determined by Goodwin in 1968 and since then it is called as The Keeler-Goodwin diagram [7]. This type of forming limit diagram is shown in Fig 1.7. The curve connecting the fracture points of each strain paths is called forming limit curve and denoted by FLC.

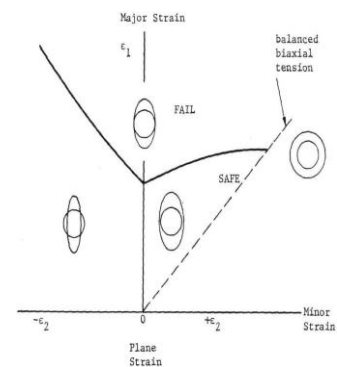


Fig 1.7 Forming Limit Diagram



### 1.6.1 Basic Understandings Concerning The Forming Limit Diagrams:

Forming Limit Diagrams represent the formability limits in the coordinate system of major ( $\epsilon_1$ ) and minor ( $\epsilon_2$ ) principal strains. The formability limit is usually characterized by the failure (rupture) and this is called as formability (fracture) limit curve. It is a very effective way of optimizing sheet metal forming. A grid of circles is etched on the surface of a sheet metal. Then the sheet metal is subjected to deformation. Usually the sheet is deformed by stretching it over a dome shaped die. Strips of different widths can be taken for the test, in order to induce uniaxial or biaxial stress state [7].

The circles deform into elliptic shapes. The strain along two principal directions could be expressed as the percentage change in length of the major and minor axes. The strains as measured near necks or fracture are the strains for failure. A plot of the major strain versus minor strain is then made. This plot is called Keeler-Goodwin forming limit diagram.

This plot gives the limiting strains corresponding to safe deformations. The FLD is generally a plot of the combinations of major and minor strains which lead to fracture. Combination of strains represented above the limiting curves in the Keeler-Goodwin diagram represents failure, while those below the curves represent safe deformations. A typical Keeler-Goodwin diagram is shown below. The safe zone in which no failure is expected is shown as shaded region. Outside this zone there are different modes of failure represented at different combinations of strains. The upper part of the safe zone represents necking and fracture.

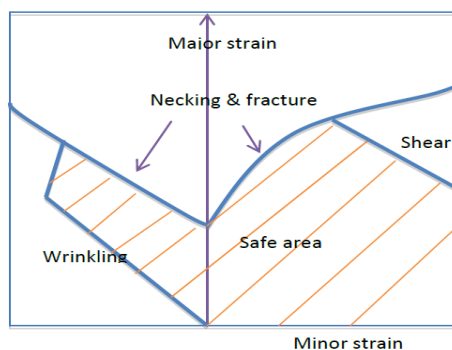


Fig 1.8: Keeler –Goodwin Diagram

The slope of the right hand side curve (necking curve) is found to decrease with increasing values of the strain hardening exponent,  $n$ . Similarly, variations in sheet thickness, composition, grain size all reduce the slope of the neck curve. The safe region is narrowed down by biaxial stress state. Sheet thickness also has effect on FLD. Higher sheet thickness increases the FLD.

### 1.7 Introduction Of Residual Stress

#### 1.7.1 Definition:

Residual stresses can be defined as those stresses that remain in a material or body after manufacture and processing in the absence of external forces or thermal gradients. The total stress experienced by the material at a given location within a component is equal to the residual stress plus the applied stress [8].

$$\text{TOTAL STRESS} = \text{RESIDUAL STRESS} + \text{APPLIED STRESS}$$

#### 1.7.2 Types of Residual Stress:

Residual stresses can be characterized by the scale at which they exist within a material. Stresses that occur over long distances within a material are referred to as macro-stresses. Stresses that exist only locally (either between grains or inside a grain) are called micro-stresses. The total residual stress at a given location inside a material is the sum of all 3 types of stresses.

Type I Stresses: Macro-stresses occurring over distances that involve many grains within a material.

Type II Stresses: Micro-stresses caused by differences in the microstructure of a material and occur over distances comparable to the size of the grain in the material. Can occur in single-phase materials due to the anisotropic behavior of individual grains, or can occur in multi-phase material due to the presence of different phases.

Type III Stresses: Exist inside a grain as a result of crystal imperfections within the grain.

#### 1.7.3 Origins Of Residual Stress:

Residual stresses develop during most manufacturing processes involving material deformation, heat treatment, machining or processing operations that transform the shape or change the properties of a material. They arise from a number of sources and can be present in the unprocessed raw material. The residual stresses may be sufficiently large to cause local yielding and plastic deformation, both on a microscopic and macroscopic level and can severely affect component performance. For this reason it is vital that some knowledge of the internal stress state can be deduced either from measurements or modeling predictions.

Both the magnitude and distribution of the residual stress can be critical to performance and should be considered in the design of a component. In any free standing body stress equilibrium must be maintained, which means that the presence of a tensile residual stress in the component will be balanced by a compressive stress elsewhere in the body. Tensile residual stresses in the surface of a component are generally undesirable since they can contribute to, and are often the major cause of, fatigue failure, quench cracking and stress-corrosion cracking. Compressive residual stresses in the surface layers are usually beneficial since they increase both fatigue strength and resistance to stress-corrosion cracking, and increase the bending strength of brittle ceramics and glass. In general, residual stresses are beneficial when they operate in the plane of the applied load and are opposite in sense (for example, a compressive residual stress in a component subjected to an applied tensile load).

## 1.8 Methods of Measuring Residual Stress

### 1.8.1 Hole Drilling Method:

Hole drilling is one of the most widely used techniques for measuring residual stress. It is relatively simple, cheap, quick and versatile. Equipment can be laboratory-based or portable, and the technique can be applied to a wide range of materials and components. The principle of the technique involves the introduction of a small hole into a component containing residual stresses and subsequent measurement of the locally relieved surface strains [9].



Fig 1.9: Hole Drilling Machine

The residual stress can then be calculated from these strains using formulae and calculations derived from experimental and Finite Element Analyses. In practical terms, a hole is drilled in the component at the centre of a special strain gauge rosette. Close to the hole, the strain relief is nearly complete but the technique suffers from limited strain sensitivity and potential errors and uncertainties related to the dimensions of the hole (diameter, concentricity, profile, depth etc.), surface roughness, flatness, and specimen preparation. Incremental hole drilling improves the versatility of the technique and enables stress profiles and gradients to be measured.

### 1.8.2 Deep Hole Drilling:

This is a variation of the technique which has been developed for measuring residual stresses in thick-section components. The method was originally developed in the 1970s by Beany [10] and Zhdanov and Gonchar [11], but has undergone considerable development since [12-14]. The basic procedure involves drilling a small reference hole through the specimen and subsequent removal of a column of material, centered about the reference hole, using a trepanning technique.



Fig 1.10: Deep Hole Drilling Machine

The diameter of the reference hole is measured accurately along its length before the column is machined out. When the column is removed the stresses relax and the reference hole diameter and column dimensions change, the dimensions of the column and reference hole are then re-measured and the residual stresses calculated from the dimensional changes caused by removing the material from the bulk of the specimen. The deep-hole drilling technique has been used to measure residual stresses in thick sections of complex shape, but there is limited agreement at this stage between experimental measurements and finite element predictions.

### 1.8.3 Laboratory X-Ray Diffraction:

X-ray diffraction has become the one of the standard methods for measuring residual stress in the past few decades [15]. X-ray diffraction measures the strain or the changes in strain, from an unstressed state, by measuring the shifts in the diffraction peak due to an external or residual stress.



Fig 1.11: Laboratory XRD

The measured strains are then converted into a stresses through Hooke's law. These calculations assume a linear elastic deformation of the material. Prevey states that residual stresses determined using x-ray diffraction assume an arithmetic average of the stress in the volume of the material defined by the irradiated area. This volume may vary from square millimeters to square centimeters and is based on the depth of penetration of the x-ray beam, which is governed by the linear absorption coefficient of the material based on the type of radiation used.

In aluminum based alloys, more than 70% of the diffracted radiation comes from the top 100 microns of the material for all the most commonly used laboratory x-ray sources. Because of this shallow depth of penetration, the spatial resolution of the residual stresses will be approximately 10 to 100 times more than other stress determining stress measuring techniques such as dissection, ultrasonic, and magnetic. The depth of penetration is dependent on the type of radiation, and in practice there are limited types of useful radiation.

For example Cu-K $\alpha$  radiation, Co-K $\alpha$  radiation and Cr-K $\alpha$  radiation are some of the common types of radiation used in laboratory settings. The limited selection of laboratory x-ray tubes leads to a limited choice of crystallographic planes that can be used for the residual strain measurement. For instance {hkl} reflection planes available for aluminum using these different types of radiation where {111}, {200}, etc. are the Miller indices of the reflection planes for the material,  $2\theta$  is the Bragg angle, and Cu, Co, and Cr are the types of K- $\alpha$  radiation.

### 1.9 Heat Treatment:

Heat treatment is an operation or combination of operations involving heating at a specific rate, soaking at a temperature for a period of time and cooling at some specified rate [16].

#### 1.9.1 Annealing of Aluminum Alloys:

The annealing procedure for aluminum alloys consists of heating the alloys to an elevated temperature, holding or soaking them at this temperature for a length of time depending upon the mass of the metal, and then cooling in still air. Annealing leaves the metal in the best condition for cold working. However, when prolonged forming operations are involved, the metal will take on a condition known as "mechanical hardness" and will resist further working. It may be necessary to anneal a part several times during the forming process to avoid cracking. Aluminum alloys should not be used in the annealed state for parts or fittings [17].

## 1.10 Aluminum Alloys And Their Application In Aerospace Industry:

### 1.10.1 2xxx - Al-Cu Alloys:

- Heat treatable
- High strength, at room & elevated temperatures
- Aircraft, transportation applications
- Representative alloys: 2014, 2017, 2024, 2219, and 2195
- Typical ultimate tensile strength range: 27-62 ksi

The 2xxx series are heat-treatable, and possess in individual alloys good combinations of high strength (especially at elevated temperatures), toughness, and, in specific cases, weldability. The higher strength 2xxx alloys are primarily used for aircraft applications. These are usually used in bolted or riveted construction. [18].

Illustrations of applications for the 2xxxx series alloys include:



Fig. 1.12- Aircraft internal structure includes extrusions and plate of 2xxx alloys.

### 1.10.2 5xxx - Al-Mg Alloys:

- Strain hardenable
- Excellent corrosion resistance, toughness, weldability; moderate strength
- Building & construction, automotive, cryogenic, marine applications
- Representative alloys: 5052, 5083, and 5754
- Typical ultimate tensile strength range: 18-51 ksi

Al-Mg alloys of the 5xxx series are strain hardenable, and have moderately high strength, excellent corrosion resistance even in salt water and very high toughness even at cryogenic temperatures to near absolute zero [18]. They are readily welded by a variety of techniques, even at thicknesses up to 20 cm. As a result, 5xxx alloys find wide application in building and construction, highways structures including bridges, storage tanks and pressure vessels, cryogenic tank age and systems for temperatures as low as  $-270^{\circ}\text{C}$  (near absolute zero), and marine applications.

Alloys 5052, 5086, and 5083 are the work horses from the structural standpoint, with increasingly higher strength associated with the increasingly higher Mg content. Examples of applications for the broadly used 5xxx series of alloys include:



Fig.1.13 - High speed single-hull ships like the Proserpio employ 5083-H113/H321 machined plate





Fig.1.14 - The internal hull stiffener structure of the high-speed .

#### 1.10.3 6xxx - Al-Mg-Si Alloys:

- Heat treatable
- High corrosion resistance, excellent extrudability; moderate strength
- Building & construction, highway, automotive, marine applications
- Representative alloys: 6061, 6063, 6111
- Typical ultimate tensile strength range: 18-58 ksi

The 6xxx alloys are heat treatable, and have moderately high strength coupled with excellent corrosion resistance. They are readily welded. A unique feature is their extrudability, making them the first choice for architectural and structural members where unusual or particularly strength- or stiffness-criticality is important. Alloy 6063 is perhaps the most widely used because of its extrudability [18].

Among the most important applications for Al-Mg-Si alloys are:

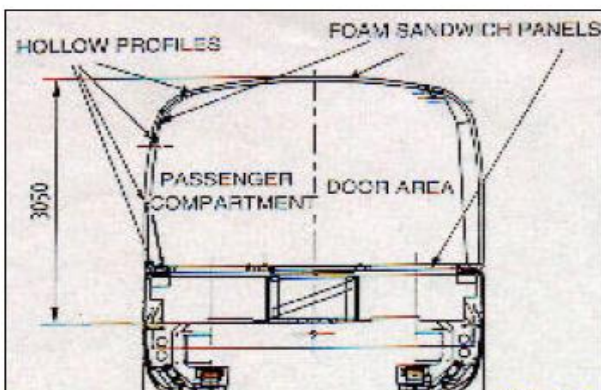


Fig 1.15: Japan employ bodies with 6061 and 6063 structural members

#### 1.10.4 7xxx - Al-Zn Alloys:

- Heat treatable
- Very high strength; special high toughness versions
- Aerospace, automotive applications
- Representative alloys: 7005, 7075, 7475, 7150
- Typical ultimate tensile strength range: 32-88 ksi

The 7xxx alloys are heat treatable and among the Al-Zn-Mg-Cu versions provide the highest strengths of all aluminum alloys. There are several alloys in the series that are produced especially for their high toughness, notably 7150 and 7475, both with controlled impurity level to maximize the combination of strength and fracture toughness.

The widest application of the 7xxx alloys has historically been in the aircraft industry, where fracture-critical design concepts have provided the impetus for the high-toughness alloy development. These alloys are not considered weldable by routine commercial processes, and are regularly used in riveted construction. The atmospheric corrosion resistance of the 7xxx alloys is not as high as that of the 5xxx and 6xxx alloys, so in such service they are usually coated or, for sheet and plate [18].

Applications of 7xxx alloys include:



Fig 1.16: Aircraft structures are of 7xxx alloy sheet or extrusion construction

In the present work, aluminum alloys 6061 and 5052 of aerospace grade has been selected in the study to analyze their formability. The formability of aluminum 6061 is analyzed only for dry condition whereas the formability of aluminum 5052 is analyzed for different tribological conditions such as dry condition, lubricant as grease and annealed condition. The 6061 alloys formability has been compared with 5052 under dry conditions. Further the formability of 5052 aluminum alloy has also been evaluated using lubricant such as grease and annealed condition. The formability under these conditions have been also compared to understand better forming conditions and analyzed for its airworthiness.

## 2. Literature Survey

Experimental and numerical evaluation of forming limit diagram for Ti6Al4V titanium and Al6061-T6 aluminum alloys sheets, Djavanroodi, A. Derogar [19]. In this work, the formability, fracture mode and strain distribution during forming of Ti6Al4V titanium alloy and Al6061-T6 aluminum alloy sheets has been investigated experimentally using a process of hydro forming deep drawing assisted by floating disc. The selected sheet material has been photo-girded for strain measurements. The effects of process parameters on FLD have been evaluated. Hill-swift and NADDRG theoretical forming limit diagram models are used to specify fracture initiation



in the finite element model (FEM) .Finally, close agreement is achieved between the experiment and numerical results for these materials. Moreover, a better fracture initiation prediction was obtained using Hill-Swift model.

Forming Limit Stress Diagram Prediction of Aluminum Alloy 5052 Based on GTN Model Parameters Determined by In Situ Tensile Test, HE Mina, LI Fuguo, and Wang Zhigang [20]. In the present study, a forming limit stress-based diagram (FLSD) has been adopted to predict the fracture limit of aluminum alloy (AA) 5052-O1 sheet. Nakazima test is simulated by plastic constitutive formula derived from the modified Gurson-Tvergaard-Needleman (GTN) model. An in situ tensile test with scanning electron microscope (SEM) is proposed to determine the parameters in GTN model. The stress and strain are obtained at the last loading step before crack. FLSD and FLD of AA5052-O1 are plotted. Compared with the experimental Nakazima test and uniaxial tensile test, the predicted results show a good agreement. The parameters determined by in situ tensile test can be applied to the research of the forming limit for ductile metals path.

Improvement of Formability and Spring-Back of AA5052-H32 Sheets Based on Surface Friction Stir Method, Sangjoon Park , Chang Gil Lee [21] .In the present work, A process to improve formability and spring-back was developed for AA5xxx-H temper sheets based on the surface friction stir (SFS) method. In the SFS method, a rotating probe stirs the sheet surface so that material flow and heat, which result from plastic deformation and friction, change the microstructure and macroscopic mechanical properties of the stirred zone and therefore, ultimately, the formability and spring-back performances of the whole sheet. When applied to AA5052-H32 sheets, the process improved formability and spring-back, as experimentally and numerically confirmed in the limit dome height. Finite element simulations based on the calculated forming limit diagrams successfully predicted the deformation of the surface friction stirred sheet including failure punch heights and failure locations in the LDH test as well as spring-back performance.

Mechanical and anisotropic behaviors of 7075 aluminum alloy sheets, Mohammad Tajally , Esmail Emadoddin [22].In this paper ,Formability of 7075 aluminum alloy sheets was studied after annealing of 71% cold worked (CW) samples at different temperatures (270–450 degC). Uniaxial tensile test, deep drawing and Erichsen test were carried out at room temperature to evaluate formability parameters. Average plastic strain ratio, planar anisotropy, and work hardening exponent of samples were calculated from the tensile test data .The formability of 7075 aluminum alloy sheets via the limit drawing ratio (LDR), Erichsen and tensile test after annealing at different temperatures was conducted. It is clear that sheets annealed at higher than 350degC possess relatively good stretchability and drawability. As a result, the formability parameters improve by increasing annealing temperature and hence formability of 7075 Al alloy could be improved

by annealing the sheets at temperatures ranges of 350–400 degC.

Formability AA5052/polyethylene/AA5052 sandwich sheets, Jian-guang LIU1, Wei XUE [23].In this paper, the formability of AA5052/polyethylene/AA5052 sandwich sheets was experimentally studied. Three kinds of AA5052/polyethylene/AA5052 sandwich specimens with different thicknesses of core materials were prepared by the hot pressing adhesive method. Then, the uniaxial tensile tests were conducted to investigate the mechanical properties of AA5052/polyethylene/ AA5052 sandwich sheets, and the stretching tests were carried out to investigate the influences of polymer core thickness on the limit dome height of the sandwich sheet. The forming limit curves for three kinds of sandwich sheets were obtained. The experimental results show that the forming limit of the AA5052/polyethylene/AA5052 sandwich sheet is higher than that of the monolithic AA5052 sheet, and it increases with increasing the thickness of polyethylene core. The limit dome height of AA5052/polyethylene/ AA5052 sandwich sheet is larger than that of monolithic AA5052 sheet. Forming limits of AA5052/polyethylene/AA5052 are higher than those of monolithic AA5052 sheet.

Using X-ray diffraction to assess Residual stresses in laser panned and welded aluminum, Brian J. Banazwski lieutenant, Rochester [24]. This thesis examines the interplay of residual stress distributions caused by welding and laser peening of aluminum alloy 5083. Residual stresses at welds in this alloy can cause fatigue and stress corrosion cracking in ship superstructures. X-ray diffraction was used to measure the residual stress distributions across welded and laser peened areas of welded aluminum plate. Full strain and stress tensors were measured and calculated in order to develop a fuller picture of the residual stress distribution in this complex geometry. The tensor analysis was found to be extremely sensitive to the exact choice of diffraction angles used in the experiment, and an algorithm was developed to optimize the design of the diffraction experiment. Bi-axial stress analysis did show an increase in compressive stress from the laser peening after a couple tenths of a millimeter followed by a gradual decrease in compressive stress as depth increases.

Influence of process parameters on the cup drawing of aluminum 7075 sheet,

G. Venkateswarlu, M. J. Davidson and G. R. N. Tagore [25].In this study, the significance of three important deep drawing process parameters namely blank temperature, die arc radius and punch velocity on the deep drawing characteristics of aluminum 7075 sheet was determined. The combination of finite element method and Taguchi analysis was used to determine the influence of process parameters. Simulations were carried out as per orthogonal array using DEFORM 2D software. Based on the predicted deformation of deep drawn cup and analysis of variance test, it was observed that blank temperature has greatest influence on the formability of aluminum material followed by punch velocity and die arc radius.

### Effect of Material and Process Variability on the Formability of Aluminum Alloys,

S. Hazraa, D. Williams, R. Roy, R. Aylmor and A. Smith [26]. This study set out to investigate the effect of material and process variations in the stamping process of AA6111-T4 and AA5754-O, with particular emphasis on the effect of tooling temperature. The temperature of parts that were manufactured in serial production was measured and was found to be between 28°C and 55°C. The effects of the parameters were tested in plane strain using the LDH test. The mean response of AA5754-O was found to be higher than for AA6111-T4, implying that it was more formable than AA6111-T4. Material properties were found to have an effect on the formability of both materials. For AA6111-T4, it was the only parameter that significantly affected its formability. AA5754-O was also found, in particular, to be affected by the temperature of the tooling.

Formability and microstructure of AA6061 Al alloy tube for hot metal gas forming at elevated temperature, HE Zhu-bin, FAN Xiao-bo<sup>1</sup>, SHAO Fei<sup>1</sup>, ZHENG Kai-lun, WANG Zhi-biao<sup>1</sup>, YUAN Shi-jinn[27]. In the present work, Free bulging test was carried out at different temperatures ranging from 350 °C to 500 °C to evaluate the formability of AA6061 extruded tube, which can provide technology foundation for complex structures forming in hot metal gas forming (HMGF) process. Maximum expansion ratio (MER) and bursting pressure were obtained to evaluate directly the formability at heated conditions. Aluminum bursting pressure decreases monotonously from 4.4 MPa to 1.5 MPa as temperature increases. The maximum expansion ratio increases firstly and reaches the maximum value of about 86% at 425 °C, then begins to drop to 65% at 500 °C. The ideal forming temperature range of AA6061 Al alloy tube for hot metal gas forming is from 400 °C to 450 °C.

Warm Forming of Aluminum Alloy 2024 at Different Temperatures, W. J. Ali O. Th. Jumah [28]. In the present study, Forming of aluminum sheets at warm forming temperatures has been investigated as an alternative manufacturing process for improving formability compared with forming at room temperature. However, the forming technology should be developed to increase the application field, especially in the predication of formability and the failure in order to design the process and die outcomes. The formability is increased for the tested sheet metals with the temperatures, and a more formability improvement is found in the (Al-2024-O) sheet metal compared with (Al-2024-T3). The formability and flow stress of (Al-2024-T3) sheet metal is good at moderate temperature until 175 °C. The possibility to form it at moderate elevated temperature with acceptable formability and higher strength for structural parts is better if compared to the annealed state (Al-2024-O).

### Formability Analysis of AA6061 Aluminum Alloy at Room Temperature,

D. Loganathan, and A. Gnanavelbabu [29]. This study focuses on the effect of annealing at different soaking temperature with furnace cooling conditions. Effects are investigated at three orientations 0°, 45°, and 90° to the rolling direction of sheet metal. The value of plastic strain ratio and strain hardening exponent at three orientations were evaluated. The normal anisotropy value increases, with respect to soaking temperature, yields good forming. Optimum annealing temperature of 413°C and 2 hrs 30 min soaking yields low tensile strength, yield strength and strength coefficient. Annealing process increases the percentage of elongation, and strain hardening exponent value. The result of physical and mechanical properties of AA6061 is good at annealing temperature 413°C and 2 hrs 30 min soaking than as-received condition. therefore Formability of AA6061 T4 mainly depends upon the physical and mechanical properties of the materials.

Analysis of forming process of automotive aluminum alloys considering formability and spring back ,wonoh lee<sup>1</sup>, Daeyong Kim, Junhyung kim, kwansoo chung and Seung hyun hong [30]. In this work, Formability and spring back of the automotive aluminum alloy sheet, 6K21-T4, were numerically investigated based on the modified Chaboche model. The Erichsen test was carried out to partially obtain forming limit strains and FLD was also calculated based on the M-K theory to complete the FLD. The failure location during simulation was determined by comparing strains with FLD strains. To verify the numerical method, the hood outer panel was stamped and compared with numerical predictions. The numerical results showed good agreement with experimental results.

Formability and Mechanical Property of 5052 Aluminum Sheets Locally Surface- Modified by the Concept of Surface Friction Joining ,Chang Gil Lee<sup>1</sup>, Sung-Joon Kim, Heung Nam Han and Kwansoo Chung[31]. In this study, Formability and mechanical property of Al sheets whose surface was locally modified by the concept of SFJ (Surface Friction Joining) were analyzed. It is noteworthy that the formability of the surface-modified sheets is greatly improved compared with base sheets. The formability is improved as the tool diameter is increased. It is found that more plastic deformation is accommodated at modified region during LDH test. Formability of the locally surface-modified 5052 aluminum alloy sheets is superior to that of the base metal, due to the fact that the locally surface-modified region can accumulate strain more than the base metal. Local surface-modification using the concept of Surface Friction Joining is considered to be the useful tool for the aluminum alloy sheet forming.

Experimental Study on the Evaluation of Necking and Fracture Strains in Sheet Metal Forming Processes, G. Centeno, A.J. Martinez-Donaire, C. Vallengano, L.H. Martinez-Palmeth, D. Morales, C. Suntaxi, F.J. Garcia-Lomas[32] , In this paper the formability of AA2024-T3 metal sheets is experimentally analyzed under different

forming processes: stretching, Stretch-bending and single point incremental forming. The conventional formability limits were correctly set from a series of normalized Nakazima tests by using different specimen geometries. The results exhibit the importance of the accuracy in the setting of the formability limits as well as the variability that these limits present depending on the forming process or some variables such as the tool radius.

Finite element simulation of deep drawing of aluminum alloy sheets at elevated temperatures, G. Venkateswarlu, M. J. Davidson and G. R. N. Tagore [33]. In this study, forming of two different aluminum alloys 6061 and 7075 has been simulated for circular cup drawing in the temperature range 50-500°C using DEFORM-2D. The results show that forming at elevated temperature can yield significant increase in product height, especially for aluminum 7075. The deep drawing of aluminum 6061 alloys show very good formability in a temperature range between 150-250°C and 400-500°C for aluminum 7075. Both the metals gave identical cup heights when drawn at 475°C. It has been confirmed that higher cup depth is possible at elevated temperatures. Forming limit and necking location has been successfully predicted in the simulation. The optimum temperature at which both the blanks will have identical maximum uniform cup depths has been found during deep drawing.

Analysis of the Increased Formability of Aluminum Alloy Sheet Formed Using Electromagnetic Forming, Imbert, J, Worswick, M., Winkler, S, Golovashchenko [34]. This paper presents an analysis of the tool\sheet interaction and how it affects the formability of the sheet. Experimental and numerical work was carried out to determine the details of the forming process and its effects on formability, damage evolution and failure. It has been determined that when the sheet makes contact with the tool, it is subject to forces generated due to the impact, and very rapid bending and straightening. The predictions indicate that relatively little damage is generated in the process except in specific areas of the parts. Damage measurements agree with the predicted trends and fractographic analysis shows that parts formed with the EM process do not fail in pure ductile failure, but rather in a combination of plastic collapse, shear fracture and ductile failure. It is concluded that the rapid impact, bending and straightening that results from the tool/sheet interaction is the main cause of the increased formability observed in EM forming. The tool/sheet interaction produces a non-plane stress condition, very high strain rates and highly non-linear strain paths.

Formability of twin roll cast 5xxx alloy sheet for automotive applications, Murat dündar, Yücel birol and A.S. akkurt [35]. An attempt was made, in the present work, to characterize the formability of the twin-roll cast AA5XXX alloy sheets further by employing forming limit diagrams and other standard formability assessment tests. The results of the earlier work on the micro structural and mechanical characterization of the Twin-Roll Cast (TRC) 5XXX alloys by the authors were encouraging and the

strip-cast AA5052 and AA5182 alloys were shown to have equivalent or superior mechanical properties and better corrosion resistance with respect to their DC-Cast and Hot Rolled counterparts. Therefore, response of TRC 5052, 5754 and 5182 alloy sheets under more complex strain states, as encountered in industrial press forming operations was determined with the concept of Forming Limit Diagrams (FLD) in the present study. Identical tests were also conducted for their Direct-Chill Cast (DCC) and hot/cold rolled counter parts. Comparing the DCC 5182 with the TRC 5052, better forming properties of the TRC 5052 originate from the same type of material characteristics which dictate the operating deformation mechanism during forming.

A method for direct measurement of multiaxial stress-strain curves in AA5182 sheet metal, T. Foecke, Iadicola, lin and S.W. Banovic [36]. In this study, A novel methodology for measuring multiaxial, in-plane stress-strain curves in AA5182 sheet metal has been presented. The strain state method is imposed using a modification of the Marciniak in-plane biaxial stretching test. Balanced biaxial stress-strain curves were measured in 5182 aluminum alloy sheet samples, and the Resulting stresses are measured using a modified X-ray diffraction (XRD) residual stress measurement system. Comparison of results are done to the strengths and hardening exponents of the same material measured in uniaxial tension in the RD and TD of the sheet. This method is currently being applied to determine how the yield locus varies for a number of different alloys as a function of plastic strain and multiaxial restrains.

Investigation of chemical composition on widely used Al6061-T6511 engineered material: An XRD analysis towards improvement of mechanical properties, Sivarao, Nur Izan T.J.S. Anand, Fairuz Dimin [37]. This work will utilize X-ray diffraction analysis to provide aid to look into the properties of the alloy, its chemical compound and alloying elements analysis to determine its benefits. XRD is the most direct and accurate analytical method for determining the presence and absolute amounts of mineral species in a sample. XRD analysis indicates that Al 6061-T6511 to contain high score rating of Si when compared to traces of Co<sub>2</sub> and Ti. The score rating from the XRD analysis revealed that the alloy contained approximately the same amount Si and Mn<sub>5</sub> with a slightly higher presence of Mn<sub>5</sub> to Si comparatively. High amounts of Mn<sub>5</sub> obtained from the XRD analysis shows that the Al 6061-T6511 has high corrosion resistance and good ductility. XRD could only indicate elements present in an alloy relative to others around micro constituents; on the other hand, XRF can accurately quantify the elements in the alloy.

Investigations on forming of aluminum 5052 and 6061 sheet alloys at warm temperatures, S. Mahabunphachai, M. Koch [38]. In the present work, deformation characteristics of Al5052 and Al6061 were investigated. In the first part of this study, material behavior of Al5052 and Al6061 sheet alloys were investigated under different process



(temperature and strain rate) and loading (uniaxial vs. biaxial) conditions experimentally. With the biaxial, hydraulic bulge tests, flow stress curves up to 60–70% strain levels were obtained whereas it was limited to ~30% strain levels in tensile tests. In the second part, the effect of the temperature and the pressure on the formability was further investigated in a set of closed-die warm hydro forming experiments. Finally, in the third part of the study, FE modeling findings and comparison with closed-die hydro forming experiments based on the material flow stress curves from both bulge and tensile tests at different temperature, pressure and strain rate conditions indicated that, in general, flow curves from both bulge and tensile tests are in good agreement with experimental .

### 3 .EXPERIMENTAL WORK

#### 3.1 Introduction To Present Work:

In the present work, A6061-T6 and A5052-H32 aerospace grade alloys have been selected .the chemical composition and the mechanical properties of the alloys are obtained from the tensile test by using UTM.Further the formability analysis is done by using a erichsen cupping test on an erichsen cupping machine to analyze the material formability .For a better understanding of the forming behavior of these materials FLD diagrams for A6061-T6 alloy and A5052-H32 alloy sheets have been studied. The effects of process parameters on FLD diagram have been evaluated and compared. The residual stresses have been analyzed after cupping test under grease condition and annealed condition to understand the stresses left over in the material after forming.

#### 3.2 Chemical Composition Table Of A6061-T6 And A5052-H32 Alloys:

TABLE 3.1: CHEMICAL COMPOSITION OF ALLOYS

Alloy	Mg	Cr	Cu	Fe	Mn	Si	Zn	others total	others each
6061	1.122	0.169	0.273	0.33	0.070	0.725	0.018	0.15	0.05
5052	2.2-2.8	0.15-0.35	0.1	0.4	0.1	0.25	0.1	0.15	0.05

#### 3.3 Mechanical Properties Of A6061-T6 And A5052-H32 Aerospace Grade Alloys:

##### MATERIAL OPTIONS:

SAMPLE 1: 200\*40\*1.8mm

SAMPLE 2: 200\*40\*1.8mm

Sample type=rectangular bar

Area=28.615mm<sup>2</sup>

Gauge length= 50mm

Final gauge length=54.35mm

#### 3.3.1 Tensile Testing:

The 2 samples of each alloy of dimension 200\*40\*1.8 mm are examined for the tensile test using Universal testing machine. The gauge length of the samples is 50mm and the final gauge lengths are 54.35 at room temperature. Stress-strain plots were obtained and ultimate tensile strength and percentage elongation values were calculated.



Fig 3.1 Sample size for the tensile test

TABLE 3.2: MECHANICAL PROPERTIES OF THE ALLOYS

PROPERTY	Al 6061	Al5052
Ultimate tensile stress	207MPa	135MPa
Elongation	16	8.7
Hardness	75	47
Break load	5.8KN	3.87KN



Fig 3.2: Tensile Test Machine

#### 3.4 Preparation of Samples:

The aluminum alloy sheets are been cut under shearing machine. The formability analysis of Al 5052 –H32 sheet is done under dry, lubricant and annealed conditions. Whereas Al-6061-T6 alloys is tested only for dry condition. The sample sizes of both alloys are shown in the table 3.3.



Fig 3.3: Shearing machine

Table 3.3: Sample Sizes of A5052 And A6061 Alloys Under Different Conditions

ALLOY	DRY CONDITION SAMPLES	LUBRICANT CONDITION SAMPLES	ANNEALED CONDITION SAMPLES
5052	70*70*1.8mm-3	70*70*1.8mm-3	70*70*1.8mm-3
	70*50*1.8mm-3	70*50*1.8mm-3	70*50*1.8mm-3
	70*30*1.8mm-3	70*30*1.8mm-3	70*30*1.8mm-3
6061	70*70*1.8mm-3		
	70*50*1.8mm-3		
	70*30*1.8mm-3		



Fig 3.4: Test samples

After cutting the samples of both alloys in to required size, the samples are screen printed to measure the strain values on forming. a screen printed sample is shown in the figure below.

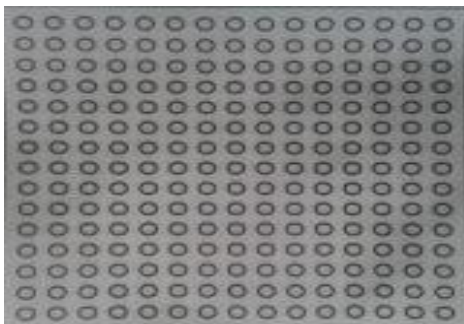


Fig 3.5 Screen printing sample

### 3.5 Heat Treatment Of The Samples:

In the present work, Annealing is to be done to the 9 samples of 5052 alloy, In order to test the material for formability under annealed condition. Annealing is carried out in an electric resistance furnace. The test pieces are annealed by heating at a temperature of 340 °C and soaking them at this temperature for 1 hour and then furnace cooled. The annealed sample is shown in fig3.7.



Fig 3.6: Electric furnace



Fig 3.7: Design of punch and die

### 3.6. Erichsen Cupping Method

#### 3.6.1 Testing Equipment:

The Erichsen cupping test shall be carried out on an erichsen cupping machine equipped 'with a die, punch and blank holder with dimensions and tolerances as shown in the figure. The construction of the machine shall be such that it is possible to observe the outside of the test piece during the test to be able to determine the instant when a through crack appears. A through crack is a crack which goes through the full thickness of the test piece and is just sufficiently wide to allow light to pass through part of its length. The machine shall be equipped with a gauge for measuring the movement of the punch with a scale division of 0.1 mm.



Fig 3.8 Erichsen cupping machine

The die, the blank holder and the punch shall be sufficiently rigid not to deform appreciably during the test. The punch shall not turn during the test. The working surface of the punch shall be spherical and polished. This spherical portion shall be in contact with the test piece during the test.

The distance from the axis of the die to the centre of the spherical part of the punch shall be less than 0.1 mm throughout its range of movement in use. The surfaces of the blank holder and of the die in contact with the test piece shall be plane and perpendicular to the axis of movement of the punch. These surfaces shall be parallel within 0.01 mm. The machine shall ensure holding the test piece with a constant holding force of approximately 10 KN. Measurement of the movement of the punch takes place from the point where it initially touches the surface of the test piece.

### 3.6.2 testing Conditions:

From literature survey, it is seen that formability depends on different testing conditions. Tribological conditions have been taken for the 5052 alloy to improve the formability of material whereas the 6061 alloy is tested only for the dry condition.

### 3.7 Formability Testing Of Samples:

#### 3.7.1 Formability Testing Of A6061 Samples:

The test carried out under controlled conditions shall be made at a temperature of 23 °C. The dimension of the first test piece is 70\*70\*1.8mm. The test piece is clamped between the blank holder and the die. The blank holder force shall be approximately 10 kN. The punch is to be brought down without shock into contact with the test piece and the measurement of penetration from this point is made. Further the test is preceded with forming the cup smoothly.



Fig 3.9 A6061 formed sample of 70\*70 mm size



Fig 3.10 A6061 formed sample of 70\*50mm size



Fig 3.11 A6061 sample of 70\*30 mm size

Towards the end of the operation, the speed is reduced to the vicinity of the lower limit in order to determine accurately the moment when a through crack appears. Finally terminate the movement of the punch at the instant when a crack appears through the full thickness of the test piece. Measure the depth of penetration. This depth expressed in millimeters is the value of the Erichsen cupping index IE.

The same procedure is followed for the remaining samples of A 6061-T6 samples and the erichsen cup height are measured.

#### 3.7.2 Formability Testing Of A5052 Samples:

The formability testing of the aluminum 5052 samples are tested by erichsen cupping test same as the samples of A6061 but the A5052 samples are tested for tribological conditions such as dry condition, grease condition and annealed condition. The formability under all these conditions have been evaluated. The residual stresses developed in the material after cup forming have been also evaluated for grease and annealed condition.

#### 3.7.3 Formability Test Of A5052 Under Dry Condition:

The same procedure of A6061 samples is followed for the 5052 samples under dry condition. All the 9 samples of dry condition are tested for formability. Terminate the movement of the punch at the instant when a crack appears through the full thickness of the test piece. Measure the depth of penetration. This depth expressed in millimeters is the value of the Erichsen cupping index IE.



Fig 3.12: A5052 Dry sample of 70\*70mm size



Fig 3.13: A5052 Dry sample of 70\*50mm size



Fig 3.14: A5052 Dry sample of 70\*30 mm size



### 3.7.4 Formability Test Of A5052 Under Lubricant Condition:

The same procedure of dry conditioned samples is repeated for the lubricant conditioned samples. But Before operating the machine, lightly grease the two faces of the test piece and the punch with grease. All the 9 samples are greased and tested for formability. Terminate the movement of the punch at the instant when a crack appears through the full thickness of the test piece. Measure the depth of penetration. This depth expressed in millimeters is the value of the Erichsen cupping index IE.



Fig 3.15:A5052 Lubricant sample of 70\*70mm size



Fig 3.16:A5052 Lubricant sample of 70\*50mm size



Fig 3.17: A5052 Lubricant sample of 70\*30mm size

### 3.7.5 Formability Test Of A5052 Under Annealed Condition:

The same procedure of lubricant conditioned samples is repeated for the annealed samples. All the 9 samples which are heat treated are tested for formability. Terminate the movement of the punch at the instant when a crack appears through the full thickness of the test piece. Measure the depth of penetration. This depth expressed in millimeters is the value of the Erichsen cupping index IE.



Fig 3.18 A5052 Annealed sample of 70\*70mm size



Fig 3.19 A5052 Annealed sample of 70\*50mm size



Fig 3.20 A5052 Annealed sample of 70\*30 mm size

### 3.8 Erichsen Cupping Index $I_e$ :

In the present work, the formability of A6061 and A5052 samples are tested using erichsen method, the cup is formed till the initiation of necking on the test piece. This cup height is taken as the formability index. This is called the erichsen cupping index. The height of the cup is measured using the vernier height gauge. The cup heights of all the samples are measured and graphs are plotted.



Fig 3.21: Vernier Height Gauge

### 3.9 Forming Limit Diagram:



Fig 3.22: Electronic Microscope



Fig 3.23: Sample testing on electronic microscope

The forming limit curve is plotted by measuring the major strain and minor strain values of formed samples of both alloys. To analyze the strain and deformation results, the formability samples are electronically microscopied and these microscopic samples are analyzed in a software UTHSCSA. therefore, major strain and minor strain values are examined from the software. therefore the forming limit diagram are plotted for both alloys.

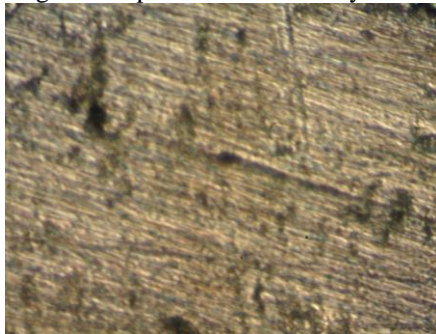


Fig 3.24: Microscopic sample of A6061 Dry sample



Fig 3.25: Microscopic sample of dry A5052

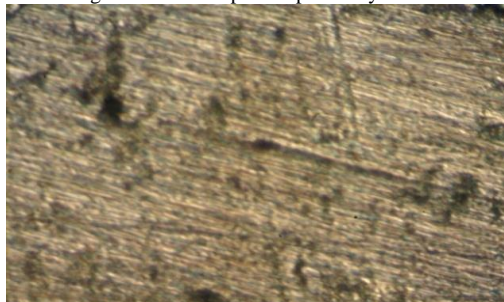


Fig 3.26: Microscopic sample of Lubricant Al5052

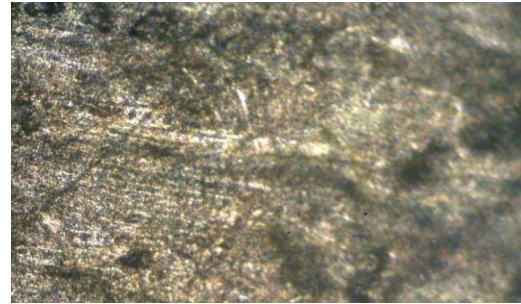


Fig 3.27 :Microscopic sample of Annealed A5052

### 3.10 Residual Stress Measurement Of A5052 Samples:

The aluminum 5052 samples of grease and annealed are tested for the residual test by XRD x-ray diffraction method using Proto Manufacturing Laboratory Non-Destructive Residual Stress Measurement System. A software analysis named XRDWin 2.0 is done which displays residual stress values on  $d$  vs.  $\sin^2 \psi$  plot.

#### 3.10.1 X-Ray Diffraction Method:

##### 1. X-ray Diffraction Equipment Overview:

X-ray diffraction (XRD) is used in this thesis to measure the residual stresses of 5052 samples. The XRD equipment used in this work is a Proto Manufacturing Laboratory Non-Destructive Residual Stress Measurement System. It has a MG2000L goniometer that rotates the XRD goniometer in the  $\psi$  -direction. A separate mounting table rotates the specimen in the  $\psi$  -direction and can automatically move the specimen. The analysis software, XRDWin 2.0, is a windows based package that has the capability to analysis and display  $d$  vs.  $\sin^2 \psi$  using a wide variety of curve fitting models for the peak profile analysis.

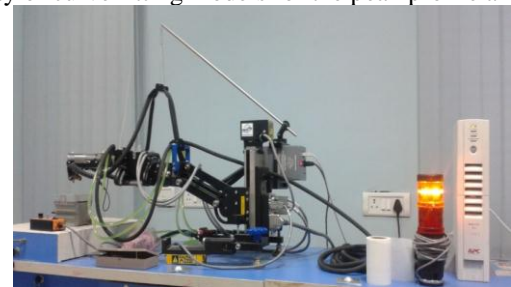


Fig 3.28: X-ray Diffraction Equipment



Fig 3.29: XRD equipment with XRD win 2.0 software

##### 2. Specimen Set-up and Orientation:

The formed annealed specimen of Al5052 is mounted on a metal block of the equipment. This mounting arrangement was used to achieve a stable placement in the

XRD. The formed annealed sample is placed in longitudinal direction to perform the residual stress test.



Fig 3.30: XRD testing for annealed sample

3. X-ray Tube Selection:

The choice of the type of x-ray radiation to use is a balance between depth of penetration and availability of a sufficiently strong diffraction peak within the appropriate angular range for the x-ray diffractometer. The present work exclusively used the copper tube with Cu-Ka radiation for all measurements.



Fig 3.31 Cu-Ka tube for testing

4.  $\psi$  Angle Selection:

Angles of  $\psi$  were chosen to give a symmetric and wide range of  $\sin^2 \psi$  values when viewed on on d vs.  $\sin^2 \psi$  plot. The x-ray diffractometer used single-exposure technique at multiple  $\psi$  -tilts with two position sensitive detectors. Cu-Ka radiation has a wavelength of 1.542nm and using the {422} reflection of aluminum, which is faced-centered cubic, the lattice parameter and the Miller indices of h=4, k=2, and l=2 .The XRDwin 2.0 software needed a minimum of eleven  $\psi$  angles per each position detector in order to calculate the stresses at a given location.

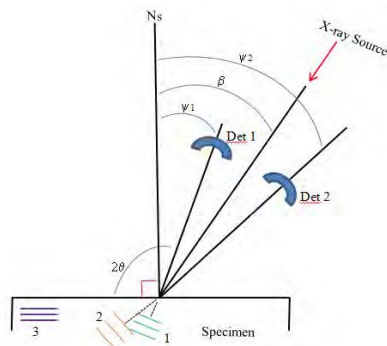


Fig 3.32: Specimen and detector

In the present work, for the Al5052 annealed sample, 13  $\psi$  angles are recorded .and a continuous peak is attained shown in the below fig3.33. The residual stress is measured using the distance between crystallographic planes, i.e., d-spacing, as a strain gage and  $\psi$  angle. As 2 detectors are used, the readings of d spacing and  $\sin^2 \psi$  are shown in detector 1 and detector 2 in the below table. Therefore the residual stress for the annealed sample is obtained.

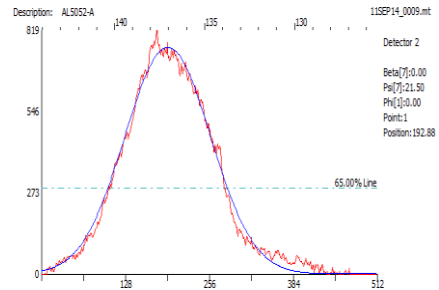


Fig 3.33: Peak distribution of annealed XRD sample

Table 3.4: D Spacing And  $\sin^2 \psi$  Values Of Annealed Sample:

DETECTOR 1		DETECTOR 2	
$\sin^2 \psi$	DSpacing	$\sin^2 \psi$	DSpacing
0.0000	0.828941	0.4651	0.829432
0.0101	0.828682	0.3659	0.828554
0.0316	0.828489	0.2927	0.827954
0.0675	0.828515	0.2195	0.827927
0.0732	0.828474	0.2104	0.827977
0.1227	0.828627	0.1464	0.828439
0.1343	0.828674	0.1343	0.828456
0.1464	0.828461	0.1227	0.828711
0.2104	0.828901	0.0732	0.828752
0.2195	0.829007	0.0675	0.828756
0.2927	0.829061	0.0316	0.828814
0.3659	0.828923	0.0101	0.828950
0.4651	0.829078	0.0000	0.828593



3.10.2 Residual Stress Test For The Aluminum 5052 Grease Sample:

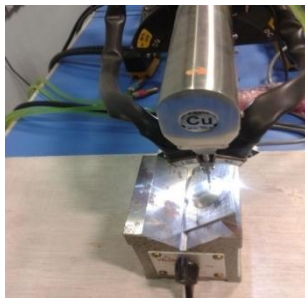


Fig 3.34: XRD testing for grease sample

The same procedure is repeated for the residual stress testing of grease sample using XRD measurement and XRD win 2.0 software. 13  $\psi$  angles were recorded and so as the d spacing of the grease sample. The continuous peak attained is shown below and the data of d spacing and  $\sin^2 \psi$  are shown the table below.

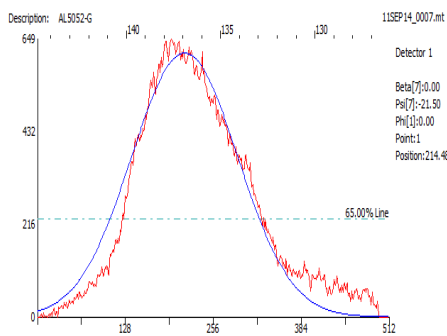


Fig 3.35 : peak distribution of grease sample

Table 3.5: D Spacing And  $\sin^2 \psi$  Values Of Greased Sample:

DETECTOR 1		DETECTOR 2	
$\sin^2 \psi$	DSpacing	$\sin^2 \psi$	DSpacing
0.0000	0.827897	0.4651	0.828131
0.0101	0.828681	0.3659	0.828651
0.0317	0.829246	0.2927	0.828744
0.0675	0.829155	0.2195	0.828761
0.0731	0.829059	0.2105	0.828665
0.1228	0.828833	0.1463	0.828370
0.1343	0.828853	0.1343	0.828275
0.1463	0.828718	0.1228	0.828205
0.2105	0.829123	0.0731	0.828117
0.2195	0.829107	0.0675	0.828128
0.2927	0.829457	0.0317	0.828636
0.3659	0.829806	0.0101	0.828996
0.4651	0.830038	0.0000	0.828914

4. RESULTS AND DISCUSSIONS

4.1 Erchsen Cup Index:

The erichsen cupping test has been carried out for the A6061-T6 and A5052-H32 samples. The test on the samples is carried out until the necking of fracture and

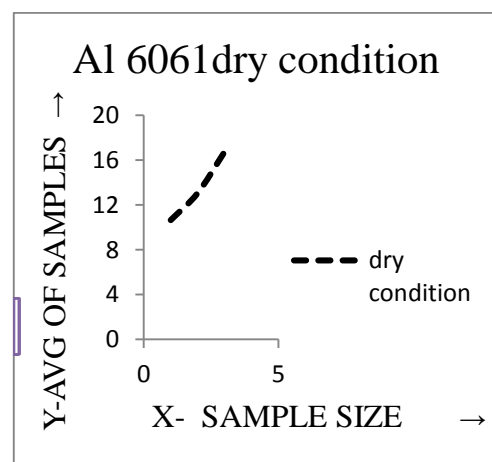
the cup height is measured by using vernier height guage. The erichsen index has been recorded and presented in the below tables.

4.2. Erchsen Cup Index Of A6061 Samples:

The erichsen cup height of A6061 samples are shown in the table 4.1. 9 samples are chosen for testing .3 samples of 70\*70mm size, 3 samples of 70\*50mm size and 3 samples of 70\*30 mm size. Graph is plotted to measure the cup height.

Table 4.1: Erichsen Index Values Of A6061 Dry Condition Samples

Sample size	Sample 1	Sample 2	Sample 3	Average
1	10.6	10.66	10.7	10.65
2	13	13	13.2	13.06
3	16.52	16.82	16.9	16.74



Graph 4.1: A6061 dry samples- sizes versus heights

The graph plotted above is between the sample sizes on the x-axis and the erichsen index on the y-axis. From the graph above, it is seen that sample size 70\*70 is having less cup height .As the sample size is changing, the erichsen index is changing .therefore it shows that the sample size is also having effect on erichsen index..Sample size 70\*30 mm is having the high erichsen index.

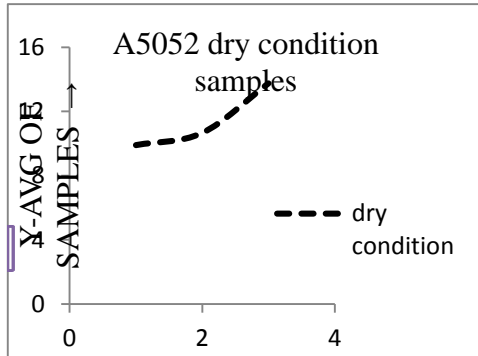
4.3 Erchsen Cup Index Of A5052 Samples:

4.3.1 Erichsen Index Of A5052 Samples For Dry Condition:

The erichsen cup heights of samples under dry condition are shown in the table 4.2. 9 samples are chosen for dry condition .3 samples of 70\*70mm size, 3 samples of 70\*50mm size and 3 samples of 70\*30 mm size. A graph is plotted to measure the cup height.

TABLE 4.2: ERICHSEN INDEX VALUES OF 5052 DRY SAMPLES

Sample size	Sample 1	Sample 2	Sample 3	Average
1	9.9	9.9	9.9	9.9
2	10.38	10.94	10.66	10.66
3	12.88	14.6	13.74	13.74



Graph 4.2: A5052 dry samples- sizes versus heights

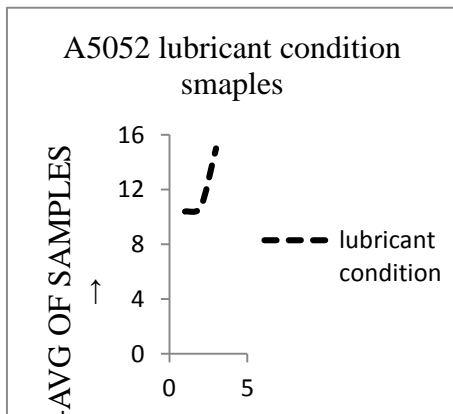
The graph plotted above is between the sample sizes on the x-axis and the erichsen index on the y-axis. From the graph above, it is seen that sample size 70\*70 is having less cup height .as the sample size is changing, the erichsen index is changing .therefore it shows that the sample size is also having effect on erichsen index. Sample size 70\*30 mm of dry condition is having the high erichsen index.

4.3.2 Erichsen Index of A5052 Samples For Lubricant Condition:

The erichsen cup height of samples under lubricant condition are shown in the table 4.3 .9 samples are chosen for lubricant condition .3 samples of 70\*70mm size ,3 samples of 70\*50mm size and 3 samples of 70\*30 mm size graph is plotted to measure the cup height.

TABLE 4.3: ERICHSEN INDEX VALUES OF 5052 LUBRICANT SAMPLES

Sample size	Sample 1	Sample 2	Sample 3	Average
1	9.95	10.84	10.39	10.39
2	10.4	10.98	10.69	10.69
3	15	15	15	15



Graph 4.3: A5052 lubricant samples- sizes versus heights

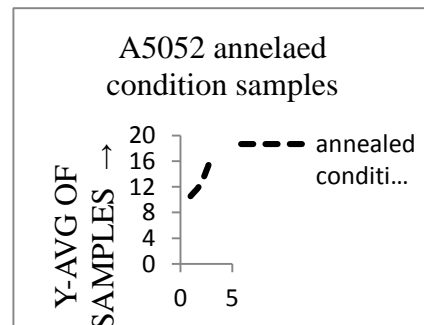
The graph plotted above is between the sample sizes on the x-axis and the erichsen index on the y-axis. From the graph above, it is seen that sample size 70\*70 is having less cup height .as the sample size is changing, the erichsen index is changing .therefore it shows that the sample size is also having effect on erichsen index. Sample size 70\*30 mm of grease condition is having the high erichsen index.

4.3.3 Erichsen Index Of A5052 For Annealed Condition:

The erichsen cup heights of samples under annealed condition are shown in the table 4.4. 9 samples are chosen for annealed condition .3 samples of 70\*70mm size ,3 samples of 70\*50mm size and 3 samples of 70\*30 mm size. A graph is plotted to measure the cup height.

TABLE 4.4: ERICHSEN INDEX VALUES OF A5052 ANNEALED SAMPLES

Sample size	Sample 1	Sample 2	Sample 3	Average
1	10.5	10.56	10.53	10.53
2	12.54	12.54	10.54	12.54
3	16.22	16.82	16.52	16.52

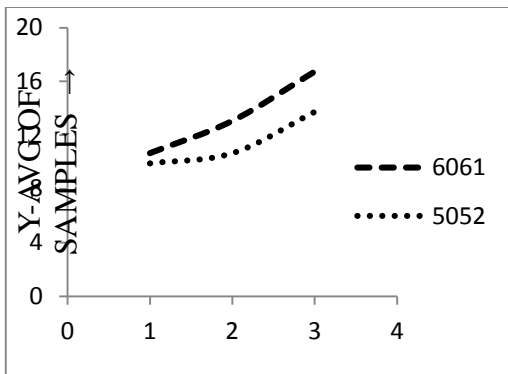


Graph 4.4: A5052 annealed samples- sizes versus heights

The graph plotted above is between the sample sizes on the x-axis and the erichsen index on the y-axis. From the graph above, it is seen that sample size 70\*70 is having less cup height .as the sample size is changing, the erichsen index is changing .therefore it shows that the sample size is also having effect on erichsen index. Sample size 70\*30 mm of annealed condition is having the high erichsen index.

4.4 Comparison Of Erichsen Index Of A6061-T6 And A5052-H32 Samples Of Dry Condition:

The erichsen cupping test have been carried out for the aerospace grade aluminum alloys of 6061 and 5052.A6061 is tested only for dry condition whereas A5052 is tested for tribiological conditions such as dry, lubricant and annealed. a graph below is plotted for the both the alloys under dry condition.



Graph4.5: Comparison of 6061 and 5052 samples – sizes versus heights

The graph plotted above is comparison of the erichsen index of Al6061 and Al5052 under dry condition between the sample sizes on the x-axis and the erichsen index on the y-axis. From the graph above, it is seen that sample size 70\*70 is having less cup height for both the alloys .as the sample size is changing, the erichsen index is changing .therefore it shows that the sample size is also having effect on erichsen index. Sample size 70\*30 mm is having the high erichsen index for both 6061 and 5052 alloys.

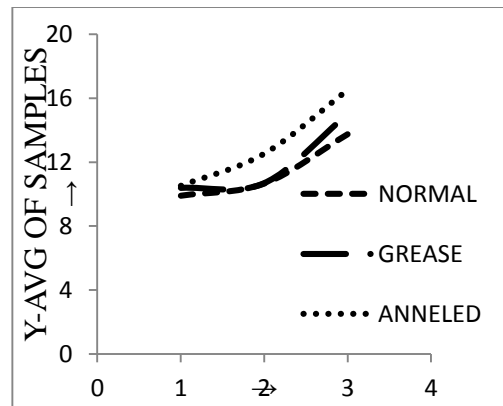
It is also observed that the 6061 is having high erichsen index than 5052 for all the samples under dry condition.therefore Al 6061 is having good formability compared with the 5052 alloy.

4.5 Comparison Of Erichsen Index Of A5052 Under Dry, Grease And Annealed Samples:

The erichsen cupping test of 5052 alloy is done under 3 conditions such as dry condition and grease as lubricant and annealed condition. The erichsen index of all the samples is reported and shown in the table 4.5.

TABLE 4.5: ERICHSEN INDEX VALUES OF A5052 DRY, GREASE AND ANNEALED SAMPLES:

Sample size	Dry samples	Lubricant Samples	Annealed Samples
1	9.9	10.39	10.53
2	10.66	10.69	12.54
3	13.74	15	16.52



Graph4.6: Comparison of 5052dry,grease ,annealed samples – sizes versus heights

The graph plotted above is the comparison of dry, lubricant and annealed condition of 5052 alloy. The graph is between the sample sizes on the x-axis and the erichsen index on the y-axis. From the graph above, it is seen that Al5052 of same size 70\*30mm is having high erichsen index under dry, grease and annealed condition.

It is also observed from the graph that annealed sample of 5052 alloy is having more E.I in comparison to other conditions of dry and grease. This can be attributed to the less residual stress developed in the material during forming.

Therefore, as the height is high, the formability of the material is high and the material can be formed easily.

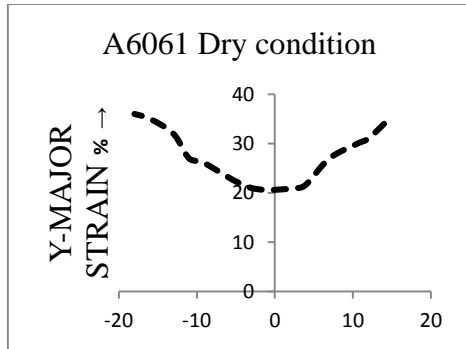
4.6 Forming Limit Diagram Of A6061 –T6alloy:

The formability of the A6061 samples are evaluated by electrically micro scoping the formed test pieces and then recording the minor strain and major strain values of the formed samples .the forming limit diagram of the A6061 under dry conditioned samples are shown in the figure 4.7 by pointing the minor strain and major strain values shown in table 4.6.

TABLE 4.6: MINOR AND MAJOR STRAIN VALUES OF A6061 SAMPLES

MINOR STRAIN%	MAJOR STRAN%
14	34
12	31
10.6	30
7	27
4.2	22
3	21
-3	21
-9	26
-11	27
-13	32
-16	35
-18	36





Graph 4.7: FLD of 6061 samples –minor strain versus major strain

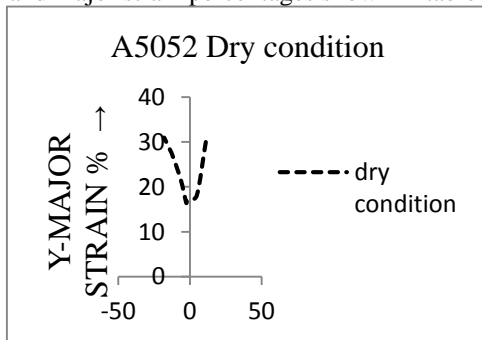
The forming limit diagram have been drawn by taking the minor strain percentage on x-axis and major strain percentage on y-axis for the samples 6061 under dry condition. The area above the curve shows the fracture and below is the safe region for the formability. The aluminum 6061 under dry condition is having formability of nearly 21%.

4.7 Forming Limit Diagram Of A5052-H32 Alloy:

The formability of the 5052 samples under dry ,lubricant and annealed condition are evaluated by electrically micro scoping the formed test pieces and then recording the minor strain and major strain values of the formed samples of all 3 conditions .the forming limit diagrams of the 5052 samples are shown in the figures below .

4.7.1 Forming Limit Diagram Of A5052 For Dry Condition:

The forming limit diagram of 5052 under dry condition is shown in fig 4.8.by pointing the minor strain and major strain percentages shown in table 4.7.



Graph 4.8: FLD of 5052 dry samples –minor strain versus major strain

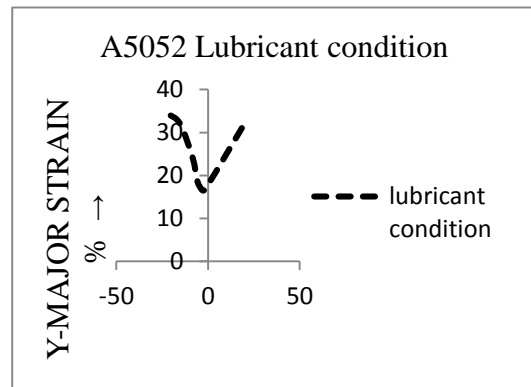
The forming limit diagram of 5052 has been drawn by taking the minor strain percentage on x-axis and major strain percentage on y-axis for the samples 5052 under dry condition. The area above the curve shows the fracture and below is the safe region for the formability. The aluminum 5052 under dry condition is having formability of nearly 17%.

4.7.2 Forming Limit Diagram Of A5052 For Lubricant Condition:

The forming limit diagram of 5052 under lubricant condition is shown in fig4.9 .by pointing the minor strain and major strain percentages shown in table 4.8.

Table 4.8: Minor And Major Strain Values Of Al5052 Lubricant Samples

MINOR STRAIN %	MAJOR STRAIN %
18.4	31
-2	16.6
-4.8	17.6
-6	19
-8.3	24
-14	31
-17	33
-20.6	34



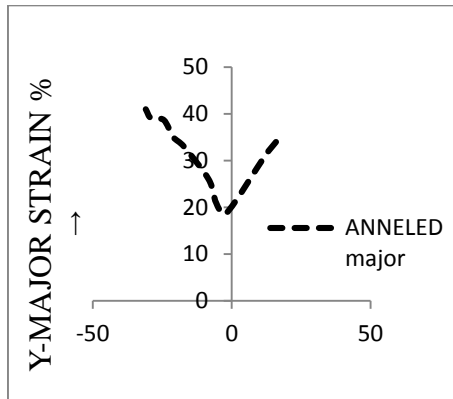
Graph 4.9: FLD of 5052 lubricant samples –minor strain versus major strainThe forming limit diagram of A5052 has been drawn by taking the minor strain percentage on x-axis and major strain percentage on y-axis for the samples 5052 under lubricant condition. The area above the curve shows the fracture and below is the safe region for the formability. The aluminum 5052 under dry condition is having formability of nearly 18.5%.

4.7.3 Forming Limit Diagram Of A5052 For Annealed Condition:

The forming limit diagram of A5052 under annealed condition is shown in fig4.10.by pointing the minor strain and major strain percentages shown in table 4.9.

TABLE 4.9: MINOR AND MAJOR STRAIN VALUES OF AL5052 ANNEALED SAMPLES

MINOR STRAIN %	MAJOR STRAIN %
16	34
12	31
-1.9	18.8
-5.6	21
-8.3	26
-17.2	33
-21	35
-24.5	38.7
-29	39
-31	41

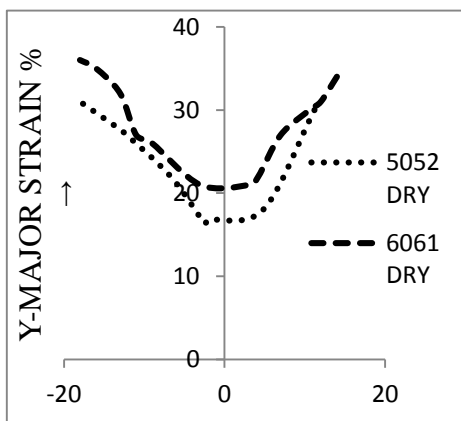


Graph 4.10: FLD of 5052 annealed samples –minor strain versus major strain

The forming limit diagram of A5052 has been drawn by taking the minor strain percentage on x-axis and major strain percentage on y-axis for the samples 5052 under annealed condition. The area above the curve shows the fracture and below is the safe region for the formability. The aluminum 5052 under annealed condition is having formability of nearly 21%.

4.8 COMPARISON OF FORMING LIMIT DIAGRAMS OF A6061 AND A5052 DRY CONDITION:

The formability of aluminum 6061 and 5052 aerospace grade alloys have been tested by erichsen cupping test and the strain values of the formed samples are electronically micros coped and recorded .the comparison of formability diagram of aluminum 6061 and 5052 under dry conditions are shown in fig 4.11.



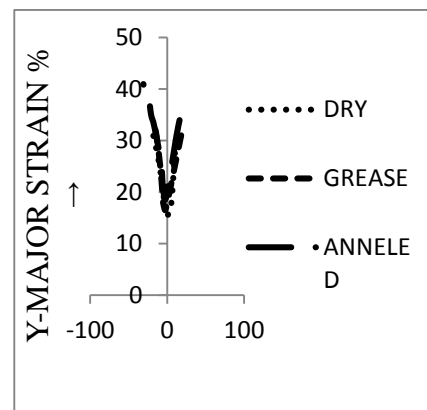
Graph 4.11:comparison of FLD of 6061 and 5052 dry samples – minor strain versus major strain

The forming limit diagram shown above is the comparison of dry, lubricant and annealed condition of 5052 alloy. The curve is plotted between the minor strain percentages on x-axis and major strain percentages on y-axis of all the samples of all conditions.

The forming limit curve for aluminum 6061 and 5052 under dry condition are nearly similar. It is also seen that the forming limit diagram height at the plain strain condition is higher for 6061 than for the 5052 .this clearly explains that aluminum 6061 is having the better formability than 5052 under similar condition. Therefore, the height is high, the formability of the material is high and the material can be formed easily.

4.9 Comparision Of Dry, Lubricant And Annealed Fld Heights Of A5052:

The formability testing of the 5052 is done under different conditions in order to check the strain state .The comparison of the forming limit diagram of 5052 aluminum alloy under different conditions is shown in fig 4.12.



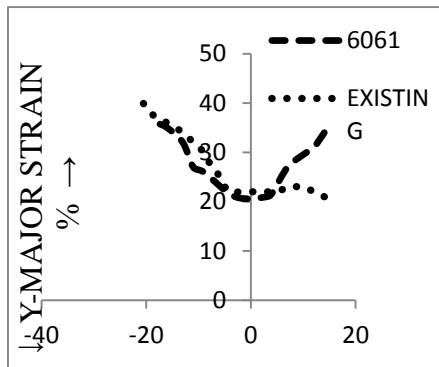
Graph 4.12: comparison of FLD of 5052 dry, grease and annealed samples –minor strain versus major strain

The forming limit diagram shown above is the comparison of dry, lubricant and annealed condition of 5052 alloy. The curve is plotted between the minor strain percentages on x-axis and major strain percentages on y-axis of all the samples of all conditions.

It is seen that the forming limit diagram height at the plain strain condition is higher for 5052 under annealed condition than for the 5052 of dry and grease condition .this clearly explains that aluminum 5052 under annealed condition is having the better formability than 5052 dry or grease condition. This can be attributed to the less residual stress developed in the material during forming. Therefore, as the height is high, the formability of the material is high and the material can be formed easily.

4.10 Comparison of Fld Of 6061alloy In Prsent Work To The Work Carried Out By F.Djavanroodi:

The forming limit diagram of aluminum 6061 of present work is compared with the existing formability investigation on 6061 alloy.



Graph 4.13: comparison of FLD of 6061 present work and 6061 existing work samples –minor strain versus major strain

The forming limit diagram have been drawn by taking the minor strain percentage on x-axis and major strain percentage on y-axis for the Al6061 of present work and the Al 6061 of the existing paper under dry condition.

It is seen that the left side of the forming limit curve is nearly similar for both present and existing work. It is also observed that the forming limit diagram height under plain strain condition is also nearly same for both the cases. The area above the curves work shows the fracture and below is the safe region for the formability. The aluminum 6061 of present work under dry condition is having formability of nearly 21% whereas the Al6061 of existing work under dry condition is having the formability of nearly 22.6%.

Therefore, it is clear that the present work is having a good relation to the existing work.

Table4.10: COMPARISION OF FLD HEIGHT ERROR:

ALLOY	PRESENT EXPERIMENTAL WORK	EXISTING EXPERIMENTAL WORK	% OF ERROR
6061	20.6	23	-10.43

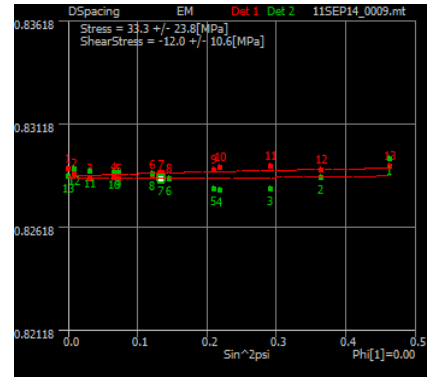
4.11 RESIDUAL STRESS ANALYSIS FOR THE 5052 SAMPLES:

The residual stress is measured by using XRD x-ray diffraction method using Proto Manufacturing Laboratory Non-Destructive Residual Stress Measurement System. a software analysis named XRDWin 2.0 is done which displays residual stress values on d vs. sin<sup>2</sup>ψ plot. The samples are tested and the results are obtained in the software.

The residual stress test is conducted for the aluminum 5052 samples under the forming condition to evaluate the stress in the sample after forming and compare the results with the forming limit diagram of 5052 samples.

4.11.1 Residual Stress For A5052 Annealed Sample:

The residual stress is measured by taking the values of d spacing and sin<sup>2</sup>ψ from the 2 detectors. A plot of d spacing and sin<sup>2</sup>ψ is shown in graph 4.14 .

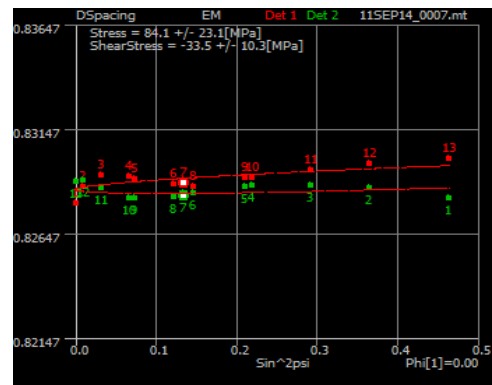


Graph 4.14: d spacing versus sin<sup>2</sup>ψ values of annealed samples

Form the above plotted graph between sin<sup>2</sup>ψ on x-axis and d spacing on y-axis, the residual stress obtained for the annealed sample is found to be +33.3 ± 23.8 MPa

4.11.2 Residual Stress For A5052 Grease Sample:

The residual stress is measured by taking the values of d spacing and sin<sup>2</sup>ψ from the 2 detectors. a plot of d spacing and sin<sup>2</sup>ψ is shown in graph 4.15 .



Graph 4.15: d spacing versus sin<sup>2</sup>ψ values of grease samples

Form the above plotted graph between sin<sup>2</sup>ψ on x-axis and d spacing on y-axis, The residual stress of the grease sample is determined by the system and is found to be +84.1 ± 23.1 MPa



## 5. CONCLUSIONS AND FUTURE SCOPE

### CONCLUSIONS:

The formability analysis on A5052-H32 and A6062-T6 alloy sheets at different conditions were examined. From the comparison of the experimental observation, the present findings are summarized as follows:

1) In this study, mechanical characteristics of A5052-H32 and A6062-T6 sheet blanks were characterized using tensile test.

2) The formability of A5052-H32 sheets were conducted using erichsen cupping method at dry condition, lubricant condition and annealed condition. For the present study at lubricant condition, grease as lubricant is used and in an effort to improve the formability of A5052, the heat treatment was developed in this work and the method was successfully applied for AA5052-H32 sheet. The erichsen cup index of A5052 samples is examined and therefore the annealing samples showed enhanced good formability compared to other conditions.

3) The formability of A6062-T6 base sheet was conducted using erichsen cupping method. The erichsen cup index of A6061 samples were examined and in comparison to erichsen index of A5052 dry condition samples, A6061 is having the high erichsen index. Therefore, A6061 possess good formability compared to A5052.

4) The forming limit diagrams of A5052 samples at dry, lubricant and annealed condition were examined. In comparison of A5052 samples at different conditions, annealed condition possess good formability. The residual stress for the A5052 samples of grease condition and annealed condition was carried out on XRD data using  $d$  vs.  $\sin^2\psi$  technique. The results showed that A5052 annealed sample is having less residual stress compared to A5052 grease sample. Therefore the less residual stresses examined in the annealed sample is a good validation to the high FLD height obtained in annealed sample. As residual stresses are less in A5052 annealed component, the components formed with annealed condition will provide better services during operating conditions.

5) The forming limit diagrams of A6061 dry samples were examined. The forming limit height of the A6061 dry sample is high in comparison to the A5052 dry samples. Therefore the A6061 samples showed enhanced good formability compared to the A5052. The present experimental forming limit diagram work of A6061 is compared with the existing experimental forming limit diagram work of A6061-T6 work carried out by F. D. Javanroodi, "Experimental and numerical evaluation of forming limit diagram for Ti6Al4V titanium and Al6061-T6 aluminum alloys sheets", Materials and Design 31 (2010) 4866–4875. Finally, close agreement is achieved between the experimental work and the existing work for the A6061-T6.

### Future Scope:

The formability of aluminum alloys 5052 and 6061 can be studied also under different conditions other than grease and the residual stress can be measured for all conditions and other forming process can be analyzed for other lubricants also. The flying hours of the aircraft component of actual flying can be recorded and compared for the components manufactured under different forming conditions.

### REFERENCES

- [1] www.aircraft materials, processes and hardware.com
- [2] Www. Aalcoaluminum 6061 Metals Ltd, Surrey KT11 3DH.com
- [3] Www Amari Aerospace Ltd, 5052 metals Cobham, Surrey, KT11 3DH.com
- [4] Richard Gedney, "Advanced materials and processes", SAE, august 2002.
- [5] Erichsen, "Mechanical testing of metals" –Modified erichsen cupping test - sheet and strip, august 1993.
- [6] www.Introduction to sheet metal forming process, SimTech Simulation, 2001.
- [7] A.P.T.M.J. Lamberts, "Effect of EDT on Formability of Aluminum Automotive Sheet", September – December 2005.
- [8] www.protomanufacturing, automated residual stress analysis.com.
- [9] N. S. Rossinia, M. Dassistia, K. Y. Benyounis and A. G. Olabib, "Methods of Measuring Residual Stresses in Components", SEM, Bethel 2005.
- [10] M.R. Hill, "Determination of residual stress based on the estimation of Eigen strain", USA: Stanford University; 1996.
- [11] A.T. DeWald, "Measurement and modeling of laser penning residual stresses in geometrically complex specimens", USA: University of California; 2005.
- [12] M.E. Kartal, C.D.M. Liljedahl, S. Gungor, L. Edwards, M.E. Fitzpatrick, "Determination of profile of the complete residual stress tensor in a VPPA weld using the multi-axial contour Method", Acta Materialia 2008; 56: 4417–4428.
- [13] R. Gunnert, "Method for measuring residual stresses and its application to a study of residual Welding stresses", Stockholm: Almqvist & Wiksell 1955.
- [14] J. Schwaighofer, "Determination of residual stresses on the surface of structural parts", Experimental Mechanics 1964; 4(2): 54–56.
- [15] By Brian j. Banazwski, "Using x-ray diffraction to assess residual stresses in laser peened and welded aluminum" December 2011
- [16] www.eisenmann.heat treatment .com
- [17] O.Henry, Heat Treating, Metals Handbook, ninth edition, ASM International, Metals Park, Volume 4, (1981).
- [18] www.aluminum, the aluminum association, inc.org.
- [19] F. D. Javanroodi, "A. Derogar, Experimental and numerical evaluation of forming limit diagram for

- Ti6Al4V titanium and Al6061-T6 aluminum alloys sheets”, *Materials and Design* 31 (2010) 4866–4875.
- [20] HE Mina, b, LI Fuguo, a, WANG Zhigang, ” Forming Limit Stress Diagram Prediction of Aluminum Alloy 5052 Based on GTN Model Parameters Determined by In Situ Tensile Test”, *Chinese Journal of Aeronautics* 24 (2011) 378-386.
- [21] Sangjoon Park, Chang Gil Lee, “Improvement of Formability and Spring-Back of AA5052-H32 Sheets Based on Surface Friction Stir Method”, *Journal of Engineering Materials and Technology*, October 2008, Vol. 130.
- [22] Mohammad Tajally, Esmail Emadoddin, ” Mechanical and anisotropic behaviors of 7075 aluminum alloy sheets”, *Materials and Design* (2010).
- [23] Jian-guang LIU<sup>1</sup>, Wei XUE, “Formability of AA5052/polyethylene/AA5052 sandwich sheets”, *Nonferrous Met. Soc. China* 23(2013) 964–969.
- [24] Brian j. Banazwski, “Using x-ray diffraction to assess residual stresses in laser peened and welded aluminum”, December 2011.
- [25] G. Venkateswarlu, M. J. Davidson and G. R. N. Tagore , “Influence of process parameters on the cup drawing of aluminum 7075 sheet”, *International Journal of Engineering, Science and Technology* Vol. 2, No. 11, 2010, pp. 41-49.
- [26] S. Hazraa, D. Williams, R. Roy, R. Aylmor and A. Smith, ” Effect of Material and Process Variability on the Formability of Aluminum Alloys”, *jmatprotec*.2011.04.001
- [27] HE Zhu -bin, FAN Xiao-b, SHAO Fei, ZHENG Kai-lun, WANG Zhi-biao, YUAN Shi-jian ,”Formability and microstructure of AA6061 Al alloy tube for hot metal gas forming at elevated temperature”, *Nonferrous Met. Soc. China* 22(2012) s364–s369.
- [28] W. J. Ali O. Th. Jumah Al -Rafidain, “Warm Forming of Aluminum Alloy 2024 at Different Temperatures”, *Engineering* Vol.20 No. 2 March 2012.
- [29] D. Loganathan, and Gnanavelbabu, “Formability Analysis of AA6061 Aluminum Alloy at Room Temperature”, *Applied Mechanics and Materials* Vol. 591 (2014) pp 55-59.
- [30] Wonoh Lee<sup>1</sup>, Daeyong Kim, Junehyung Kim, Kwansoo Chung and Seung Hyun Hong ,”Analysis of forming process of automotive aluminum alloys considering formability and spring back”, *Key Engineering Materials* Vols. 345-346 (2007) pp. 857-860.
- [31] Chang Gil Lee, Sung-Joon Kim, Heung Nam Han, and Kwansoo Chung, ” Formability and Mechanical Property of Aluminum Sheets Locally Surface-Modified by the Concept of Surface Friction Joining” ,*Advanced Materials Research* Vols. 26-28 (2007) pp. 401-404.
- [32] G. Centeno, A.J. Martinez-Donaire, C. Vallengano, L.H. Martinez-Palmeth, D. Morales, C. Suntaxi, F.J. Garcia-Lomas ,”Experimental Study on the Evaluation of Necking and Fracture Strains in Sheet Metal Forming Processes”, *Proceedings of the 5th Manufacturing Engineering Society International Conference – Zaragoza – June 2013*.
- [33] G. Venkateswarlu, M. J. Davidson and G. R. N. Tagore ,”finite element simulation of deep drawing of aluminum alloy sheets at elevated temperatures” , *ARPN journal of engineering and applied sciences* vol. 5, no. 7, July 2010 .
- [34] Imbert, J Worswick, M.Winkler, S Golovashchenko, "Analysis of the Increased Formability of Aluminum Alloy Sheet Formed Using Electromagnetic Forming," *SAE Technical Paper* 2005-01-0082, 2005.
- [35] Murat dündar, yücel biro, ” formability of twin roll cast AA5xxx alloy sheet for automotive applications”, *Advanced Materials Research*, 2007
- [36] T. Foecke, M.A. Iadicola, A. Lin, and S.W. Banovica, “Method for Direct Measurement of Multiaxial Stress-Strain Curves in Sheet Metal”, *The Minerals, Metals & Materials Society and ASM International* 2007, DOI: 10.1007/s11661-006-9044.
- [37] Sivarao ,Nur Izan T J.S.Anand,Fairuz Dimin, investigation of chemical composition on widely used Al 6061-T6511 engineered material: An XRD analysis towards improvement of mechanical properties,*International Journal of Basic & Applied Sciences IJBAS-IJENS* Vol:10 No:04 August 2010.
- [38] S. Mahabunphachai, M. Koch, Investigations on forming of aluminum 5052 and 6061 sheet alloys at warm temperatures, *Materials and Design* 31 (2010) 2422–2434